

Comparative Characterization of Indonesian AISI 316L Stainless Steel and Commercial Femoral Stem for Artificial Hip Joint Applications

Mujib Wahyudi^{1*}, Rifky Ismail²

¹ Department of Mechanical Engineering, Universitas Trunojoyo Madura, East Java, 69162, Indonesia.

² Department of Mechanical Engineering, Diponegoro University, Central Java, 50275, Indonesia.

* Corresponding Author. E-mail : mujib.wahyudi@trunojoyo.ac.id

Article information - : Received : 25-12-2025; Revised : 19-01-2026; Accepted : 26-01-2026

Abstract

The development of the femoral stem, part of the artificial hip joint, requires a material with microstructures, mechanical properties, and chemical composition that meet the requirements of a medical implant. This study aims to characterize and compare Indonesian AISI 316L stainless steel with two commercial femoral stem implants used by patients, namely XYZ products from the United States and ABC products from India. The tests carried out on the three products include tensile tests, macro hardness, microhardness, microstructure observations, and chemical composition analysis. The tensile test results show that XYZ products have the highest ultimate tensile strength (UTS) of 1065.6 ± 11.7 MPa, while the Indonesian AISI 316L (IDN) and ABC products showed lower UTS values of 580.9 ± 0.3 and 536.3 ± 9.4 MPa, respectively. Microhardness tests showed that XYZ products achieved the highest hardness value of 306.0 ± 13.5 VHN with an increasing hardness gradient towards the surface. Meanwhile, the Indonesian AISI 316L materials showed a relatively homogeneous hardness distribution with an average value of approximately 197.5 ± 1.3 VHN. Observation of microstructures reveals differences in grain size and distribution, which correlate with microhardness values. Analysis of the elemental composition shows that all three materials exhibit characteristics of austenitic stainless steel with variations in the alloy element content. Overall, the results highlight the influence of microstructural features and alloy composition on mechanical performance. Although the Indonesian AISI 316L material evaluated in this study is not classified as implant-grade stainless steel, the findings provide a baseline reference for future material development. It emphasizes the need for strict compliance with implant-grade standards, manufacturing optimization, and surface treatment to enable potential application in femoral stem component.

Keywords: orthopedic implant; austenitic alloy; tensile behavior; hardness distribution; microstructure.

1. Introduction

An artificial hip joint is one of the engineering products that is widely used to treat joint damage due to fractures, osteoarthritis, and other degenerative diseases [1]. The femoral stem components of artificial hip joints must have a combination of corrosion resistance, mechanical properties, and good compatibility to be able to function optimally in the long term in the human body.

There are several types that have been used as artificial hip joint materials, including titanium (Ti) alloys, cobalt-based alloys, and stainless steel [2]-[4]. Among these materials, AISI 316L austenitic stainless steel is still widely used because it has good corrosion resistance, adequate mechanical strength, and relatively lower production costs than other materials [5], [6]. Therefore, AISI 316L is still the top choice, especially for developing countries.

In Indonesia, until now there are no commercially produced artificial hip joint products in the country. All the needs of artificial hip joints are still met through imported products, which has an impact on high costs and dependence on foreign manufacturers. This condition encourages the need for research that focuses on the development of implant materials based on national resources and manufacturing capabilities.

Several previous studies have addressed the mechanical and microstructural characterization of AISI 316L for biomaterial applications [6]-[9]. However, studies that directly compare local AISI 316L materials with commercial femoral stem products that have been used in patients are still very limited, especially in the context of the readiness of local Indonesian materials. Therefore, this study proposes a comparative characterization between

local AISI 316L and commercial femoral stem implants as the scientific basis for the development of artificial hip joints made in Indonesia.

Femoral stem implants used in clinical applications are typically manufactured from implant-grade stainless steel. Implant-grade stainless steel such as 316L vacuum melted (VM), which complies with ASTM F138 or ISO 5832-1 standards employed to ensure controlled chemical composition, high cleanliness, and improved biocompatibility. In contrast, the AISI 316L stainless steel investigated in this study is a commercially available material sourced from a local Indonesian manufacturer and does not claim compliance with implant-grade standards. Therefore, this research is positioned as a comparative and preliminary characterization study. It focuses on evaluating the mechanical properties, microstructure, and chemical composition of locally sourced AISI 316L stainless steel in comparison with commercial femoral stem implants. The results are expected to provide a baseline reference for assessing the potential of local materials and for guiding future development toward implant-grade requirements.

2. Experimental Methods

2.1. Material

This research uses three types of materials. The first material is a commercial femoral stem which is hereinafter referred to as XYZ products originating from the United States. The second material is a commercial femoral stem referred to as an ABC product that originated in India. Both implant products were obtained from post-operative patients in collaboration with orthopedic specialists. The third material is local AISI 316L stainless steel purchased from Tira Austenite Manufacturing, Indonesia which is hereinafter referred to as IDN products. The comparison shown in this study is therefore intended to evaluate differences in mechanical properties, microstructure, and chemical composition between locally sourced AISI 316L stainless steel and retrieved commercial femoral stem implants, rather than perform a direct performance equivalence assessment.

Based on the manufacturer specification datasheet provided by Tira Austenite Manufacturing, the local AISI 316L stainless steel (IDN) contains iron (Fe) as the base element with a composition of 65.29 wt.%. The major alloying elements consist of chromium (Cr) 17.80 wt.%, nickel (Ni) 11.40 wt.%, and molybdenum (Mo) 2.55 wt.%, which are essential for corrosion resistance and mechanical performance. Minor elements include carbon (C) 0.03 wt.%, silicon (Si) 0.98 wt.%, manganese (Mn) 1.90 wt.%, phosphorus (P) 0.035 wt.%, and sulfur (S) 0.015 wt.%. The nominal chemical composition of the IDN material is summarized in [Table 1](#).

Table 1. Chemical composition of local AISI 316L stainless steel (IDN) based on manufacturer specification data sheet

Element	Fe	C	Si	Mn	P	S	Cr	Mo	Ni
Composition (wt. %)	65.29	0.03	0.98	1.90	0.035	0.015	17.80	2.55	11.40

2.2. Mechanical Testing

Tensile testing is carried out to determine the ultimate tensile strength (UTS), yield strength, and elongation values of each material. Young's modulus was not evaluated in this study because the focus was placed on the comparative assessment of strength and ductility, which are more critical parameters for evaluating the load-bearing performance of femoral stem materials. In addition, the elastic modulus of austenitic stainless steels such as AISI 316L is well established in the literature and generally exhibits limited variation among similar grades. The tensile test specimen is manufactured to the JIS Z2201 standard and tested using a universal testing machine (UTM). For each material, two specimens were tested to ensure repeatability of the results.

Macro hardness was performed to evaluate the overall surface hardness of the materials using a Vickers hardness method with a Controlab testing machine, referring to the ASTM E18 standard. Four measurements of hardness were conducted on each specimen, and the reported microhardness value represents the average of these measurements. Microhardness testing was conducted to evaluate the distribution of hardness at the microscale using a Vickers microhardness method in accordance with the ASTM E384 standard. The measurements were carried out using a Shimadzu HMV-M3 microhardness tester. Three testing positions

(positions 1, 2, and 3) were selected from the inner region toward the outer surface of the femoral stem specimen, as schematically illustrated in Figure 1. The measured microhardness values were used to analyze the hardness gradient across the specimen cross-section.

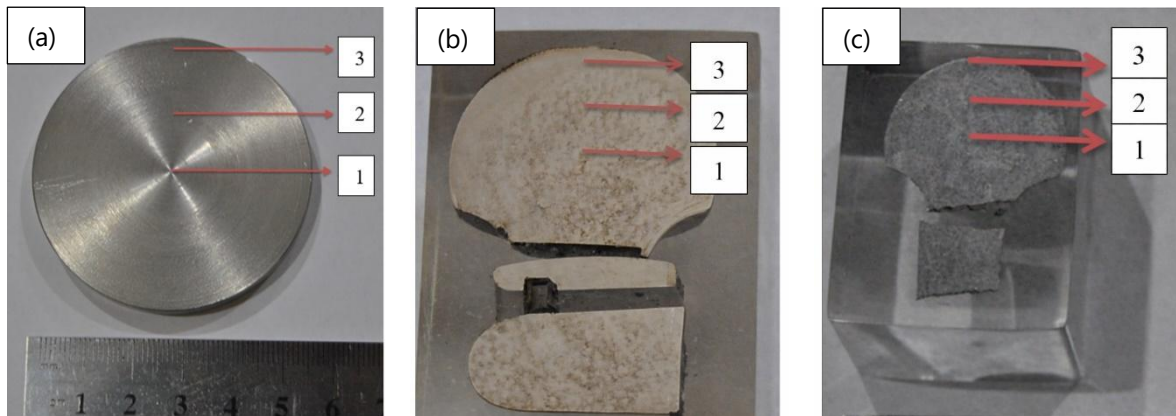


Figure 1. Schematic illustration of microhardness testing positions from the inner region (position 1) toward the outer surface (position 3) of the (a) IDN, (b) ABC, and (c) XYZ femoral stem specimens

2.3. Microstructure Observation

Microstructure observation was conducted to examine the grain morphology and phase distribution of the materials. Prior to observation, all specimens underwent standard metallographic preparation procedures, including sectioning, mounting, grinding, polishing, and chemical etching. Sectioning was performed to obtain representative cross-sections of each material, followed by mounting in resin to facilitate handling during preparation. Grinding was completed using silicon carbide (SiC) abrasive papers with progressively finer grit sizes, followed by polishing using diamond paste to obtain a mirror-like surface finish.

Chemical etching was performed using Glyceregia reagent to reveal the austenitic grain structure of the stainless-steel specimens. The etching process was carefully controlled to ensure consistent contrast and clear grain boundary definition for all samples. Microstructural observations were achieved using an optical metallurgical microscope (Olympus PME 3 series). For each material (XYZ, ABC, and IDN), observations were completed at three different positions, corresponding to the same locations used in the microhardness testing, viz. position 1 (core region), position 2 (intermediate region), and position 3 (near-surface region), as illustrated in Figure 1. This approach allows a direct correlation between microstructural features and the local microhardness distribution. The microstructures observed of the three materials were then compared in terms of grain size, grain distribution, and phase characteristics to support the interpretation of the mechanical and microhardness test results.

2.4. Elemental Composition Analysis

An analysis of the composition of the elements is executed to identify the chemical element content of each material. The analysis was performed using optical emission spectroscopy (OES), which is commonly applied for quantitative chemical analysis of stainless-steel alloys. Specimens with flat and clean surfaces were prepared prior to testing to ensure accurate measurement results. For each material, one representative specimen was analyzed, and the elemental composition was recorded in weight percentage (wt.%). The obtained results were then compared to the standard chemical composition requirements of AISI 316L stainless steel. The comparison was intended to evaluate material conformity and to assess the similarity between local AISI 316L material and commercial femoral stem implants.

3. Results and Discussion

3.1. Tensile Test

The results of tensile testing on the three materials, to wit IDN products (local AISI 316L), ABC products (commercial implants from India), and XYZ products (commercial implants from the United States), are shown in Figure 2. The parameters analyzed include yield strength, UTS, and elongation.

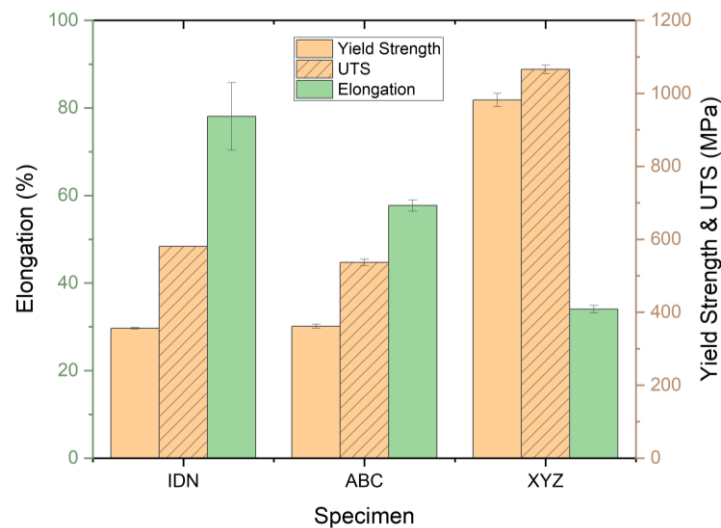


Figure 2. Tensile test results of IDN, ABC, and XYZ specimens. The bars represent mean values obtained from two specimens, and the error bars indicate the corresponding standard deviations

Based on the test results, the yield strength value of IDN material was 356.14 ± 2.1 MPa, while ABC products showed almost the same value, which is 361.5 ± 6.2 MPa. The similarity of yield strength values shows that the ability of two materials to resist initial plastic deformation is relatively equal. On the other hand, XYZ products have a much higher yield strength value, which is 981.7 ± 18.1 MPa. This remarkably high yield strength may be associated with strain hardening mechanisms induced by intensive plastic deformation during the manufacturing process. Previous studies on AISI 316L stainless steel have demonstrated that cold working processes, such as rolling, can significantly increase yield strength through the combined effects of increased dislocation density, work hardening, and the possible formation of strain-induced martensite [10], [11]. In addition, microstructural strengthening mechanisms related to refined grain structures and dense dislocation networks have also been reported to effectively restrict dislocation motion. Thus, it contributes to elevated yield strength in 316L stainless steel [12]. These strengthening mechanisms provide a reasonable explanation for the substantially higher yield strength observed in the XYZ product compared to the IDN and ABC materials.

In the UTS parameter, the XYZ product also showed the highest value of 1065.6 ± 11.7 MPa. Meanwhile, IDN and ABC products have UTS values of 580.9 ± 0.3 and 536.3 ± 9.4 MPa, respectively. This difference in UTS values indicates that XYZ products can withstand greater maximum loads before the occurrence of failure. This condition again indicates the strong influence of the manufacturing process and mechanical treatment applied to commercial implants compared to local AISI 316L materials.

The elongation value indicates the behavior of ductility as opposed to tensile strength. IDN material has the highest elongation value of $78.1 \pm 7.7\%$, followed by the ABC product at $57.7 \pm 1.3\%$. However, the XYZ product has the lowest elongation value of $34.0 \pm 0.8\%$. The high elongation value of IDN material implies an excellent degree of ductility. It shows an important characteristic for implanted materials to accommodate deformation and dynamic loads in the human body without experiencing brittle failure.

Largely, the tensile test results show a trade-off relationship between strength and ductility in all three materials. The IDN product exhibits mechanical behavior representative of untreated or solution-annealed AISI 316L stainless steel, characterized by moderate strength and high ductility. In contrast, the XYZ and ABC products

show indicative mechanical characteristics of treated or thermomechanical processed materials, with enhanced strength but reduced ductility. These findings highlight the significant influence of manufacturing history on the mechanical performance of femoral stem implants. The results also support the potential of Indonesian AISI 316L as a baseline material for further development through controlled processing and surface modification.

3.2. Hardness Test

3.2.1 Macro hardness

The results of macro hardness testing as shown in Figure 3. The macro hardness values were measured using the Rockwell A scale (HRA), where HRA represents the Rockwell hardness number obtained using a diamond cone indenter under a specific minor and major load configuration. This hardness scale is suitable for evaluating materials with relatively high surface hardness.

The IDN product exhibited an average macro hardness value of 64.5 ± 0.5 HRA, which is comparable to that of the XYZ product at 64.0 ± 0.7 HRA. In contrast, the ABC product showed a significantly lower macro hardness value of 55.2 ± 0.2 HRA. The similar macro hardness values observed for the IDN and XYZ products indicate comparable resistance to surface indentation at the macro scale, despite the substantial differences in their tensile strength and ductility.

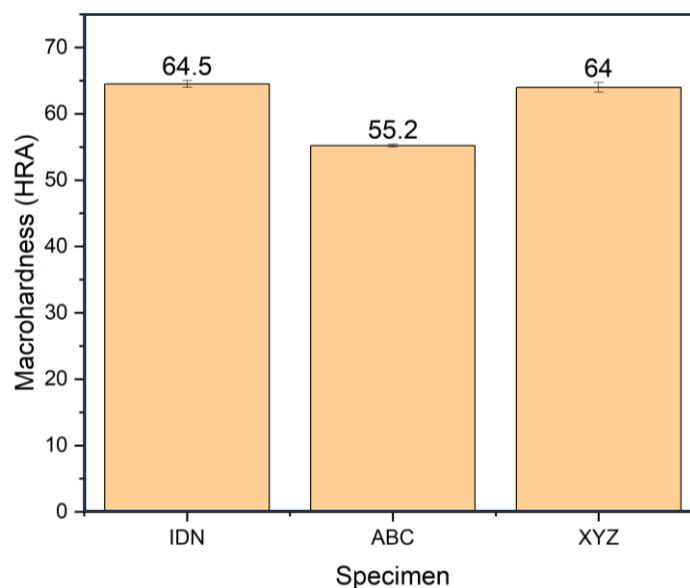


Figure 3. Macro hardness test results of IDN, ABC, and XYZ specimens

The relatively high macro hardness values of IDN and XYZ materials suggest that both materials have better resistance to surface plastic deformation than ABC products. Low macro hardness values in ABC products may signal that the material has a lower level of plastic deformation or work hardening or has a softer microstructure at the macro scale [10]-[12].

Macro hardness testing reflects the overall surface hardness influenced by bulk mechanical properties and near-surface conditions, rather than localized microstructural variations. Therefore, the observed differences in macro hardness among the three materials are reasonably attributed to variations in processing history. In the meantime, localized hardness gradients are further examined through microhardness testing in the following subsection.

3.2.2 Microhardness

Microhardness testing was conducted to evaluate distribution of hardness across the cross-section of each material, from the inner region to the outer surface. The test was performed using the Vickers microhardness method, and the hardness values are expressed in Vickers Hardness Number (VHN). Measurements were achieved at three different positions for each specimen, position 1 (inner region), position 2 (middle region), and position 3 (outer region near the surface), as illustrated in Figure 4.

Figure 4 presents the microhardness values of IDN, ABC, and XYZ materials, including the mean value and standard deviation derived from measurements at the three positions. The IDN material exhibits a relatively uniform microhardness profile, with values of 196.0, 198.3, and 198.3 VHN at positions 1, 2, and 3, respectively, and a low standard deviation of ± 1.33 VHN. This uniformity indicates good microstructural homogeneity across the cross-section. Such homogeneity is preferred for artificial hip joint applications because it promotes uniform stress distribution, minimizes localized stress concentration, and improves long-term mechanical reliability under cyclic physiological loading conditions [13].

In contrast, the ABC product shows a noticeable variation in microhardness values across the measured positions. The hardness values increased from 116.2 VHN at position 1 to 142.6 VHN at position 3, resulting in a relatively large standard deviation of ± 14.43 VHN. This inhomogeneous hardness distribution suggests non-uniform plastic deformation or uneven mechanical treatment during the manufacturing process. Similar hardness gradients in austenitic stainless steels have been reported to originate from variations in local strain hardening and microstructural evolution during forming processes [10], [11].

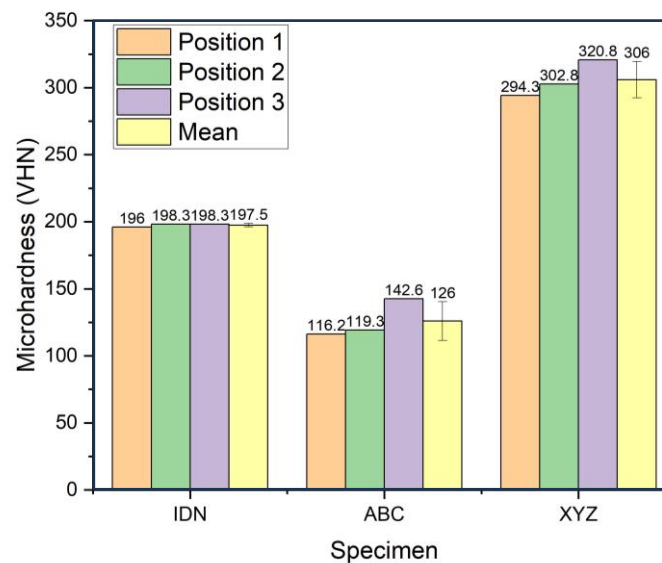


Figure 4. Microhardness test results of IDN, ABC, and XYZ specimens

The XYZ product exhibits the highest microhardness values among the three materials with values increasing from 294.3 VHN at position 1 to 320.8 VHN at position 3. The pronounced hardness gradient toward the outer surface indicates the presence of a surface hardening effect or a high degree of strain hardening induced during manufacturing. Previous studies have shown that cold working processes in AISI 316L stainless steel significantly increase hardness through dislocation multiplication, grain refinement, and strain-induced martensitic transformation, which are commonly employed in commercial implant components to enhance surface wear resistance [10]-[12].

The relatively uniform microhardness profile of the IDN material indicates that it represents an as-received AISI 316L stainless steel condition without additional mechanical or surface treatments. Therefore, the IDN material serves as a baseline reference for comparison with commercially processed femoral stem implants, which typically undergo specific mechanical and surface treatments to meet clinical performance requirements.

The error bars shown in [Figure 4](#) represent the standard deviation of microhardness values measured at the three different positions of each specimen. It reflects the hardness gradient across the cross-section rather than repeated indentations at a single point.

3.2.3 General Discussion

The increased distribution of microhardness towards the surface in XYZ products points out a gradient of mechanical properties from the inside to the outer part of the femoral stem. This gradient has the potential to provide an advantage in implant applications, where harder surfaces can increase wear resistance, while a more ductile inner is able to withstand dynamic loads [14], [15].

In contrast, the IDN material exhibits a homogeneous distribution of hardness across the cross-section, which means that the microhardness values remain relatively constant from the inner region to the surface, with only minimal variation between measurement positions. This homogeneous hardness distribution reflects a uniform microstructural condition and consistent mechanical response throughout the material. The characteristic of an as-received AISI 316L stainless steel emerges without additional mechanical or surface treatments. Such uniformity is beneficial in minimizing localized stress concentrations and ensuring predictable mechanical behavior under physiological loading conditions.

Generally, the results of macro hardness and microhardness tests show that the local AISI 316L material has adequate hardness and a homogeneous distribution of mechanical properties. Although XYZ products exhibit higher microhardness values on surfaces, IDN materials still show good potential for further development through manufacturing process optimization or surface treatment to meet the needs of artificial hip joint applications.

3.3. Microstructure Observation

Microstructure observation was executed to understand the influence of microstructure characteristics on the different microhardness values, at different test positions (position 1 to position 3) in each specimen. This analysis focused on grain size, grain morphology, and grain boundary distribution, which plays an important role in determining the mechanical properties of femoral stem material.

3.3.1 Microstructure

The results of microstructure observation at 200× magnification show that the three products have different microstructural characteristics, as shown in [Figure 5](#). Although a detailed quantitative grain size measurement was not performed, the grain size variation can be reasonably estimated based on the 50 µm scale bar, allowing a comparative analysis between different positions and products.

The IDN specimen exhibits a relatively uniform microstructure across all observed positions. The grains are predominantly equiaxed with an estimated grain size ranging from approximately 20–25 µm at both position 1 and position 3. The grain boundaries are clearly defined and evenly distributed, indicating good microstructural homogeneity. This uniform grain structure contributes to the relatively consistent microhardness values observed in the IDN specimen.

In contrast, the ABC specimen shows a non-homogeneous microstructure between different positions. At position 1, the microstructure is dominated by coarse grains with an estimated grain size exceeding 40 µm, as inferred from the scale bar in [Figure 5 \(c\)](#). Meanwhile, at position 3, the grain size appears relatively smaller, in the range of approximately 20–30 µm, accompanied by visible slip lines, as shown in [Figure 5 \(d\)](#). The presence of slip lines indicates localized plastic deformation, suggesting that the thermomechanical processing or heat treatment in the ABC specimen was not uniform throughout the femoral stem.

The XYZ specimen presents a comparatively fine grain structure, particularly near the surface. At position 1, the estimated grain size ranges from approximately 20–30 µm, whereas at position 3, the grains appear finer, with an estimated size of approximately 10–20 µm, as shown in [Figure 5 \(e\)](#) and [Figure 5 \(f\)](#). The grain refinement observed near the surface region is associated with higher microhardness values, which is consistent with the Hall–Petch relationship. It happens where finer grain sizes lead to increased material hardness.

The grain size values presented in this study are estimated based on scale bar observation and are intended for comparative purposes. Nevertheless, these estimations are sufficient to explain the observed trend in microhardness variation among different positions and specimens.

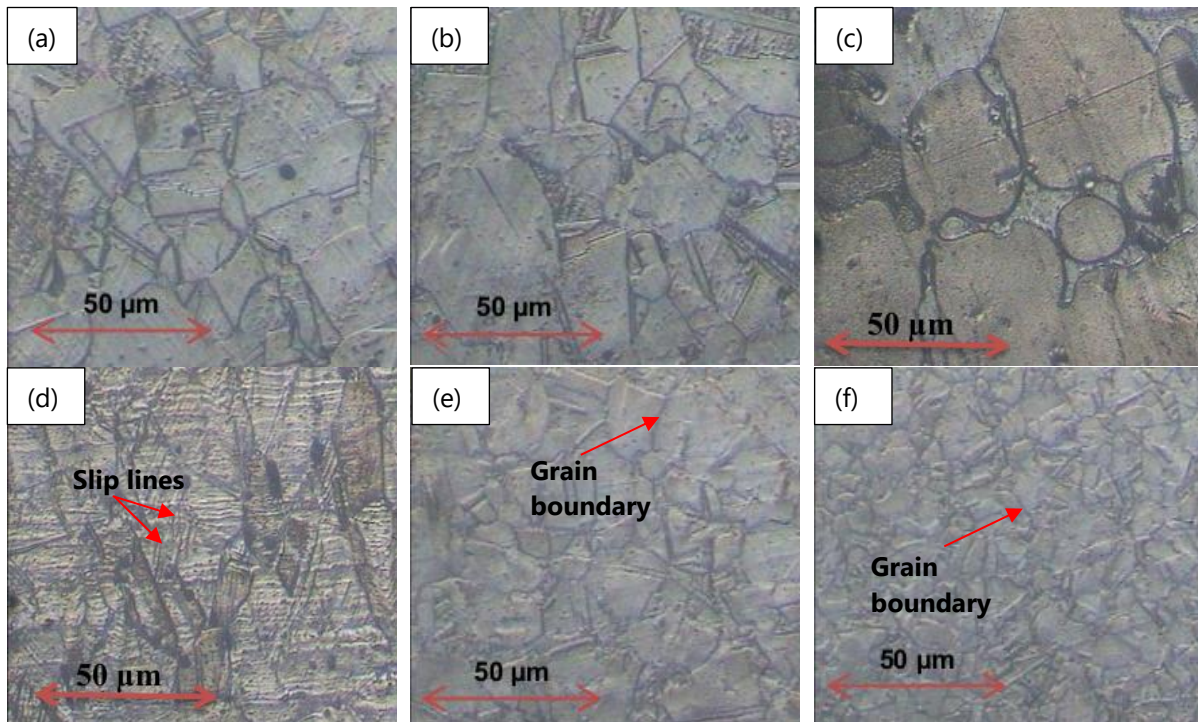


Figure 5. Microstructure of IDN, ABC, and XYZ specimens, (a) Position 1 of IDN specimen, (b) Position 3 of IDN specimen, (c) Position 1 of ABC specimen, (d) Position 3 of ABC specimen, (e) Position 1 of XYZ specimen, and (f) Position 3 of XYZ specimen

3.3.2 Correlation of Microstructure with Microhardness

The differences observed in microstructures have a strong correlation with the results of microhardness testing. Product XYZ showed an increase in microhardness value from 231.8 VHN in position 1 to 278.4 VHN in position 3. This improvement is in line with the observation of microstructures that show the grain size becoming smoother and tighter towards the surface. In accordance with Hall–Petch's Law, a decrease in grain size increases the number of grain boundaries that act as a barrier to dislocation movement, thereby increasing the hardness of the material [16], [17].

In contrast, in ABC products, the lowest microhardness value of 134.6 VHN at position 1 correlated with the coarse-grained microstructure observed in the micro image. Large grain sizes result in a lower grain boundary density, reducing the resistance to dislocation movement during plastic deformation. Consequently, dislocations can propagate more easily across the grains, leading to reduced hardness and increased material softness. The relatively higher hardness value at position 2 (202.9 VHN) suggests the presence of a localized zone that experienced higher plastic deformation or partial strain hardening compared to other regions with higher plastic deformation than other positions.

The IDN product showed a relatively constant microhardness value at all test positions, which was in the range of 196–198.3 VHN. The consistency of these values correlates with a homogeneous microstructure and relatively uniform grain size. The absence of significant differences in grain size between positions leads to an even distribution of microhardness.

In general, these results suggest that the variation in microhardness in the femoral stem is strongly influenced by microstructural characteristics, specifically grain size and grain boundary distribution. XYZ products have a microstructural gradient that results in higher surface hardness, while IDN materials show good homogeneity of

properties and have the potential to be further developed through manufacturing process optimization or surface treatment.

3.4. Analysis of the Composition of Chemical Elements

Chemical element composition analysis was performed to identify differences in the content of alloy elements in the femoral stem of XYZ product, ABC product, and local AISI 316L material (IDN product). Besides that, it was conducted to evaluate their suitability as a pelvic joint implant material. The composition of the elements plays an important role in determining the mechanical properties, corrosion resistance, and microstructural stability of austenitic stainless steel used in biomedical implants.

The ABC and XYZ specimen analyzed in this study was obtained from a retrieved femoral stem explant. The original material specification provided by the manufacturer was not available. Therefore, material classification in this study is based solely on elemental composition analysis rather than certified standard documentation.

3.4.1 Comparison of the composition of the main elements

Based on the results of the elemental composition test as shown in Table 2, the Fe element is the dominant element in all specimens, with the highest content in ABC products (66.9 wt.%) and the lowest in XYZ products (61.2 wt.%). This difference shows that there is a variation in the alloying level and manufacturing processes in each material [18].

Table 2. Results of the element composition test of IDN, ABC, and XYZ specimens

Element	Composition of stainless steel (wt.%)		
	XYZ	IDN	ABC
Fe	61.2	65.2	66.9
C	0.0288	0.0136	0.015
Si	0.263	0.421	0.277
Mn	4.58	1.9	1.58
P	0.0110	<0.0050	<0.0050
S	0.0078	0.0210	<0.0050
Cr	21.1	14.5	15.5
Mo	1.21	1.01	2.04
Ni	10.9	14.7	13.3
Al	0.0162	0.0383	<0.0020
Co	0.0251	0.420	0.0355
Cu	0.0545	0.645	0.125
Nb	0.328	0.312	0.0556
Ti	0.0225	0.0775	0.0157
V	0.0624	0.0910	0.0681
W	<0.0250	0.0324	<0.0250
Pb	0.0291	0.0983	0.0451

The Cr content of XYZ products reached 21.1%, much higher than IDN products (14.5 wt.%) and ABC products (15.5 wt.%). The high Cr content plays an important role in the formation of a passive layer of chromium oxide (Cr₂O₃) that increases corrosion resistance, especially in biological environments [19]. This indicates that XYZ products are designed with a focus on long-term corrosion resistance.

Element of Ni serves as an austenite stabilizer. IDN products have the highest Ni content (14.7 wt.%), followed by ABC products (13.3 wt.%) and XYZ products (10.9 wt.%). The relatively high Ni content of IDN products supports austenitic phase stability, which is in line with the results of microstructure observations showing uniformly equiaxed grains [20].

The Mo element contributes to increased resistance to pitting corrosion. ABC product shows the highest Mo content (2.04 wt.%), followed by XYZ product (1.21 wt.%) and IDN product (1.01 wt.%). The higher Mo content of

ABC product has the potential to increase resistance to local corrosion, although it is not offset by good microstructural homogeneity [21].

3.4.2 Carbon Elements and Their Implications for Mechanical Properties

The C content in all specimens was at a low level (<0.03 wt.%), in accordance with the characteristics of L-type (low carbon) stainless steel. XYZ products have the highest C content (0.0288 wt.%), while IDN products have the lowest content (0.0136 wt.%). The low carbon content reduces the risk of chromium carbide precipitation at grain boundaries, thereby increasing resistance to intergranular corrosion [22].

The slight variation in carbon content also contributes to differences in mechanical properties. The marginally higher carbon content in the XYZ product may contribute to increased hardness through solid solution strengthening. Additionally, the indication of strain hardening in the XYZ product is inferred from the presence of finer grains near the surface, microstructural deformation features observed in the micrographs, and a significant increase in surface microhardness. These characteristics are commonly associated with plastic deformation and work hardening in austenitic stainless steels

3.4.3 Minor and Trace Elements

The Mn element in XYZ products is relatively high (4.58 wt.%) compared to IDN products (1.90 wt.%) and ABC products (1.58 wt.%). Mn, acts as a deoxidizer, can increase mechanical strength through solid solutions. The higher Mn content of XYZ products has the potential to contribute to higher microhardness values [23], [24].

Minor elements such as Nb, Ti, V, and W were detected in small amounts in the entire specimen. These elements have the potential to form carbide or carbonitride precipitates that can affect the mechanical strength and stability of microstructures. XYZ and IDN products exhibit a relatively higher Nb content than ABC products, which can contribute to increased strength through the precipitation strengthening mechanism [25].

The content of elements S and P, which are generally detrimental to toughness and corrosion resistance, is at low levels in all materials. However, IDN products exhibit slightly higher S content (0.0210 wt.%), which concerns in the purification and quality control process of materials for medical applications.

3.4.4 Implications for Femoral Stem Applications

Taken as a whole, the results of elemental composition analysis showed that all three materials had characteristics of austenitic stainless steel with different alloying strategies. XYZ products stand out with their high Cr and Mn content, which contribute to better hardness and corrosion resistance. Based on its composition, the XYZ material shows closer similarity to high-alloy or high-nitrogen austenitic stainless steels rather than conventional AISI 316L, although definitive classification cannot be made due to the absence of manufacturer specifications.

The IDN material demonstrates compositional features that support austenitic phase stability and microstructural homogeneity; however, the relatively high sulfur content suggests that it does not fully meet implant-grade cleanliness requirements. Even though accompanied by variations in mechanical properties, the ABC material exhibits higher Mo and Ni contents, which may enhance resistance to localized corrosion. These findings indicate that while local AISI 316L material has competitive alloying potential, stricter control of raw material selection, impurity levels, and manufacturing processes are required before it can be considered suitable for femoral stem implant applications.

4. Conclusion

This study presents a comparative characterization of Indonesian AISI 316L stainless steel and two commercial femoral stem materials obtained from retrieved implants, focusing on their mechanical properties, microstructural features, and chemical composition. The XYZ material exhibits the highest mechanical performance, particularly in terms of surface microhardness and tensile strength. This behavior is strongly associated with refined grain structures near the surface and higher alloying element contents, especially chromium and manganese, which contribute to strengthening and corrosion resistance. However, due to the

absence of material certification and documented manufacturing history, the XYZ material is discussed based on its observed characteristics rather than classified under a specific implant-grade standard.

The Indonesian AISI 316L material demonstrates relatively stable mechanical behavior and a homogeneous microhardness distribution supported by a uniform equiaxed grain microstructure. Nevertheless, its chemical composition, particularly sulfur content, does not meet implant-grade requirements such as ASTM F138 or ISO 5832-1 (316LVM). Therefore, the Indonesian AISI 316L evaluated in this study cannot be classified as a medical implant material and is instead positioned as a baseline or developmental material. The ABC material, on the other hand, shows notable inhomogeneity in both microstructural and mechanical properties across different test positions, as reflected by variations in grain size and microhardness values, indicating non-uniform thermomechanical processing.

In conclusion, the results confirm that variations in grain size distribution and alloying element composition have a direct influence on microhardness behavior in austenitic stainless steels. While the Indonesian AISI 316L material investigated in this work is not suitable for direct biomedical application, the findings provide a valuable reference for future material development. Compliance with implant-grade standards, improved compositional cleanliness, optimized thermomechanical processing, and appropriate surface treatments are essential steps for enabling the potential use of locally developed stainless steel materials in femoral stem components.

5. Acknowledgments

The authors would like to thank orthopedic specialists who have helped provide post-operative femoral stem samples used in this study. The author also expressed his gratitude to Tira Austenite Manufacturing, Indonesia, for the provision of local AISI 316L stainless steel material. Appreciation was also conveyed to the Mechanical Engineering Department, Diponegoro University, for the support of laboratory facilities and research facilities used in the implementation of this study.

6. References

- [1] C. Thorson, K. Galicia, A. Burlison, O. Bouchard, D. Hoppensteadt, J. Fareed, and W. Hopkinson, "Matrix metalloproteinases and their inhibitors and proteoglycan 4 in patients undergoing total joint arthroplasty," *Clinical and Applied Thrombosis/Hemostasis*, vol. 25, pp. 1-9, 2019, doi: 10.1177/1076029619828113.
- [2] S. Prasad, V. Ratheesh, V. Manakari, G. Parande, M. Gupta, and R. Wong, "The potential of Magnesium based materials in mandibular reconstruction," *Metals*, vol. 9, no. 3, p. 302, 2019, doi: 10.3390/met9030302.
- [3] D. Avery, L. Morandini, N. Celt, L. Bergey, J. Simmons, R. K. Martin, H. J. Donahue, and R. O. Navarrete, "Immune cell response to orthopedic and craniofacial biomaterials depends on biomaterial composition," *Acta Biomater.*, vol. 161, pp. 285-297, 2023, doi: 10.1016/j.actbio.2023.03.007.
- [4] K. C. Lai, S. C. Chao, K. K. Tseng, J. W. Yeh, and P. Y. Chen, "Biocompatible as-cast and homogenized TiNbTaZrMoV high entropy alloys: mechanical properties, corrosion resistance and in vitro studies," *Journal of Materials Research and Technology*, vol. 24, pp. 9708-9721, 2023, doi: 10.1016/j.jmrt.2023.05.201.
- [5] S. Ali, M. Irfan, U. M. Niazi, A. M. A. Rani, A. Rashedi, S. Rahman, M. K. A. Khan, M. A. Alsaiari, S. Legutko, J. Petru, and A. Trefil, "Microstructure and mechanical properties of modified 316L stainless steel alloy for biomedical applications using powder metallurgy," *Materials*, vol. 15, no. 8, p. 2822, 2022, doi: 10.3390/ma15082822.
- [6] S. Attabi, A. Himour, L. Laouar, and A. Motallebzadeh, "Mechanical and wear behaviors of 316L stainless steel after ball burnishing treatment," *Journal of Materials Research and Technology*, vol. 15, pp. 3255-3267, 2021, doi: 10.1016/j.jmrt.2021.09.081.
- [7] A. M. Kumar, B. Suresh, S. Das, I. B. Obot, A. Y. Adesina, and S. Ramakrishna, "Promising bio-composites of polypyrrole and chitosan: surface protective and in vitro biocompatibility

- performance on 316L SS implants," *Carbohydrate Polymers*, vol. 173, pp. 121–130, 2017, doi: 10.1016/j.carbpol.2017.05.083.
- [8] G. Singh, Y. Lamichhane, A. S. Bhui, S. S. Sidhu, P. S. Bains, and P. Mukhiya, "Surface morphology and microhardness behavior of 316L in HAp-PMEDM," *Facta Universitatis, Series: Mechanical Engineering*, vol. 17, no. 3, pp. 445–454, 2019, doi: 10.22190/FUME190510040S.
- [9] M. A.-. Amin, A. M. A.-. Rani, M. Danish, F. T. Zohura, S. Rubaiee, R. Ahmed, S. Ali, and M. Sarikaya, "Analysis of hybrid HA/CNT suspended-EDM process and multiple-objectives optimization to improve machining responses of 316L steel," *Journal of Materials Research and Technology*, vol. 15, pp. 2557–2574, 2021, doi: 10.1016/j.jmrt.2021.09.074.
- [10] S. Tanhaei, K. Gheisari, and S. R. A. Zaree, "Effect of cold rolling on the microstructural, magnetic, mechanical, and corrosion properties of AISI 316L austenitic stainless steel," *International Journal of Minerals, Metallurgy and Materials*, vol. 25, pp. 630–640, 2018, doi: 10.1007/s12613-018-1610-y.
- [11] S. Mohammadzahi, H. Mirzadeh, M. J. Sohrabi, M. Roostaei, and R. Mahmudi, "Elucidating the effects of cold rolling route on the mechanical properties of AISI 316L austenitic stainless steel," *Materials Science and Engineering: A*, vol. 865, p. 144616, 2023, doi: 10.1016/j.msea.2023.144616.
- [12] Y. Hong, G. Yin, Y. Zheng, W. Zhang, and Z. Wei, "Mechanisms of synergistically enhanced strength and plasticity in 316L stainless steel fabricated by laser powder bed fusion via cold rolling and annealing treatments," *Materials Science and Engineering: A*, vol. 935, p. 148364, 2025, doi: 10.1016/j.msea.2025.148364.
- [13] H. Katiksiz and S. Gündüz, "Effect of grain size and deformation temperature on mechanical properties and failure Behaviour of 316L austenitic stainless steel," *Metallophysics and Advanced Technologies*, vol. 43, no. 5, pp. 673–688, 2021, doi: 10.15407/mfint.43.05.0673.
- [14] O. A. Zambrano, B. I.-. Guerrero, S. A. Rodríguez, and J. J. Coronado, "Running-in period during sliding wear of austenitic steels," *Tribology Letters*, vol. 72, p. 70, 2024, doi: 10.1007/s11249-024-01867-z.
- [15] S. M. Jafarpour, M. Mandel, L. Krüger, H. Biermann, and A. Dalke, "Functional properties of expanded austenite generated on AISI 316L by plasma nitrocarburizing using different active screen materials," *Materials Research Express*, vol. 11, no. 11, p. 116501, 2024, doi: 10.1088/2053-1591/ad898b.
- [16] D. M. Field, K. R. Limmer, and B. C. Hornbuckle, "On the grain growth kinetics of a low density steel," *Metals*, vol. 9, no. 9, p.997, 2019, doi: 10.3390/met9090997.
- [17] M. S. Anwar, R. K. Melinia, M. G. Pradisti, and E. S. Siradj, "Effect of prior austenite grain-size on the annealing twin density and hardness in austenitic stainless steel," *International Journal of Technology*, vol. 12, no. 6, pp. 1149–1160, 2021, doi: 10.14716/ijtech.v12i6.5190.
- [18] B. Blinn, M. Klein, C. Gläßner, M. Smaga, J. C. Aurich, and T. Beck, "An investigation of the microstructure and fatigue behavior of additively manufactured AISI 316L stainless steel with regard to the influence of heat treatment," *Metals*, vol. 8, no. 4, p. 220, 2018, doi: 10.3390/met8040220.
- [19] Y. Leng, D. Yang, P. Ming, B. Li, and C. Zhang, "Improvement of corrosion resistance and electrical conductivity of stainless steel 316L bipolar plate by pickling and passivation," *World Electric Vehicle Journal*, vol. 12, no. 3, p. 101, 2021, doi: 10.3390/wevj12030101.
- [20] H. Khanmohammadi, W. Wijanarko, and N. Espallargas, "The role of tribofilm chemical composition on wear of austenitic stainless steel lubricated with water-glycol containing ionic-liquids as additives," *Wear*, vol. 520–521, p. 204672, 2023, doi: 10.1016/j.wear.2023.204672.
- [21] P. M. O. Silva, M. C. C. Filho, J. A. d. Cruz, A. J. M. Sales, A. S. B. Sombra, and J. M. R. S. Tavares, "Influence on pitting corrosion resistance of AISI 301LN and 316L stainless steels subjected to cold-induced deformation," *Metals*, vol. 13, no. 3, p. 443, 2023, doi: 10.3390/met13030443.
- [22] S. A. A. Maged and R. S. Hadi, "Improved corrosion resistance in biomaterial applications of the AISI 316L alloy," *Advances in Science and Technology Research Journal*, vol. 19, no. 9, pp. 254–265, 2025, doi: 10.12913/22998624/207058.

- [23] B. Kalandyk, R. Zapała, and M. Starowicz, "The Effect of Si and Mn on microstructure and selected properties of Cr-Ni stainless steels," *Archives of Foundry Engineering*, vol. 17, no. 1, pp. 192–196, 2017, doi: 10.1515/afe-2017-0034.
- [24] R. Zhang, J. He, S. Xu, F. Zhang, and X. Wang, "The roles of Ce and Mn on solidification behaviors and mechanical properties of 7Mo super austenitic stainless steel," *Journal of Materials Research and Technology*, vol. 22, pp. 1238–1249, 2023, doi: 10.1016/j.jmrt.2022.11.148.
- [25] H. Pasiowiec, P. Ledwig, L. Ząbek, T. Kargul, P. L. Graca, M. Wojtaszek, M. Gude, R. Stanik, J. Falkus, C. Leinenbach, and B. Dubiel, "Microstructure and mechanical properties of 316L/inconel 625 gradient multi-material additively manufactured by laser powder bed fusion," *Materials & Design*, vol. 260, p. 115162, 2025, doi: 10.1016/j.matdes.2025.115162.